

Article

Kinetics Study of Gas Pollutant Adsorption and Thermal Desorption on Silica Gel

Rong A¹, Meng Liu¹, Liping Pang^{1,*}, Dongsheng Yang², Jun Wang¹ and Yue Zhou³

¹ School of Aeronautic Science and Engineering, Beijing University of Aeronautics and Astronautics, Beijing 100191, China; arong@buaa.edu.cn (R.A.); liumeng@buaa.edu.cn (M.L.); wangjun@buaa.edu.cn (J.W.)

² Beijing Spacecrafts, Beijing 100094, China; xingyewuhen@163.com

³ Aviation Key Laboratory of Science and Technology on Aero Electromechanical System Integration, Nanjing 211102, China; yuehao20103@163.com

* Correspondence: pangliping@buaa.edu.cn; Tel.: +86-10-8231-6654

Academic Editor: Peter Van Puyvelde

Received: 6 April 2017; Accepted: 8 June 2017; Published: 12 June 2017

Abstract: Silica gel is a typical porous desiccant material. Its adsorption performance for gaseous air pollutants was investigated to determine its potential contribution to reducing such pollutants. Three gaseous air pollutants, toluene, carbon dioxide, and methane, were investigated in this paper. A thermogravimetric analyzer was used to obtain the equilibrium adsorption capacity of gases on single silica gel particles. The silica gel adsorption capacity for toluene is much higher than that for carbon dioxide and methane. To understand gas pollutant thermal desorption from silica gel, the thermogravimetric analysis of toluene desorption was conducted with 609 ppm toluene vapor at 313 K, 323 K, and 333 K. The overall regeneration rate of silica gel was strongly dependent on temperature and the enthalpy of desorption. The gas pollutant adsorption performance and thermal desorption on silica gel material may be used to estimate the operating and design parameters for gas pollutant adsorption by desiccant wheels.

Keywords: silica gel; gas pollutant; adsorption kinetics; thermal regeneration; experimental analysis

1. Introduction

With the development of civil aviation transportation, passengers and crews are becoming more demanding for comfort and safety. In a cramped and crowded airliner cabin, passengers and crews have long complained about air quality problems, which have caused fatigue, dizziness, headache, ear disease, throat pain, and even occasional neurological disorders [1]. As an important issue for the cabin environment, gaseous contaminants directly influence the comfort, health, and working efficiency of passengers and crews.

The air quality in the aircraft cabin is maintained directly by the Environment Control System (ECS), which supplies fresh air into the cabin and exhausts cabin air through an outflow valve [2]. In a typical civil aircraft, the air supplied into the cabin by the ECS consists of approximately 50% outside air and 50% filtered recirculation air [3]. Usually, the High Efficiency Particulate Air (HEPA) filter for the recirculation air has an efficiency of 99.97% to remove 0.3-micrometer particles, but the HEPA filter is incapable of removing gaseous pollutants. With the innovation of “Cleaner Engine” launched globally, future civil aircrafts need more efficient engines and less bleed air [4]. In order to maintain a healthy cabin environment with a low concentration of gaseous pollutants, novel filters are being explored and developed continuously.

In recent years, researchers have conducted experimental and theoretical studies on various contaminant removal techniques, such as adsorption [5–9], photocatalytic oxidation [10–12], catalytic converters, non-thermal plasma oxidation [13], etc. Activated carbon adsorption has long been used

in cabin purification systems due to its excellent stability, limited secondary pollution, and portability. However, Metts [14] found that the adsorbed volatile organic compounds (VOCs) could react with ozone and produce secondary pollution, such as ultrafine particles, formaldehyde, and some other harmful by-products. In addition, humidity control requirements and difficulties in regenerating high-boiling point solvents and flammability may impede the application of activated carbon. Hence, activated carbon is not used in any airlines. Different alternative adsorbents need to be developed to overcome these problems.

In fact, the major requirements for a regenerative adsorbent are its adsorption capacity and its regeneration efficiency, which determine the contaminants' removal efficiency in a whole adsorption and desorption cycle. As an alternative to activated carbon, silica gel shows several advantages. Particularly, the use of silica gel in air purification is attracting more and more attention due to its high removal efficiency and stability to varying humidity levels [15–18]. An average removal efficiency up to 94% was obtained in the experiments of Fang et al. [15]. In their experiments, human subjects, flooring materials, and four pure chemicals (i.e., toluene, formaldehyde, ethanol, and 1,2-dichloroethane) were used as gas pollutants to investigate the effect of a desiccant wheel in the ventilation system. In their experiments, it was worth noting that the VOCs were nearly 100% removed from the recirculation air at about 333 K–343 K, regardless of the moisture load. The competition between VOCs and water vapor reduced when the regeneration temperature increased to 333 K–343 K. Their experiments confirmed the potential air-cleaning performance of silica, which also helps to confirm the aims of this paper. However, the desiccant wheel VOC removal capacity was far from reaching its limit during their eight-hour experiments. Further studies on the equilibrium uptake and kinetics need to be carried out to promote the investigation of silica gel air-cleaning properties. At the same time, they conducted passenger perception experiments in a simulated aircraft cabin in which the air purifier had a certain effect on improving the cabin air quality [19]. Silica gel not only adsorbs VOCs, but also ensures that the humidity of the aircraft cabin remains in a safe range. In order to simulate the silica gel adsorption and desorption processes, Zhang et al. conducted a theoretical study based on the mass conservation and diffusion equation [18]. They calculated the coefficient of convective mass transfer derived by analogy to the coefficient of convective heat transfer.

An air purification system based on a silica gel-coated desiccant wheel is shown in Figure 1. This conceived system can be extended to a ventilation system for a semi-enclosed cabin, such as an aircraft cabin, basement, tank or armored vehicle. In this example, the exhaust air out of the cabin is divided into two parts: regeneration air and recirculation air. The recirculation air is purified first by a high-efficiency filter and then by a desiccant wheel. In an air mixing unit, the purified air is mixed with the fresh air cooled by an ECS, and then returned to the cabin. In addition, the regeneration air is heated to regenerate a part of the desiccant wheel.

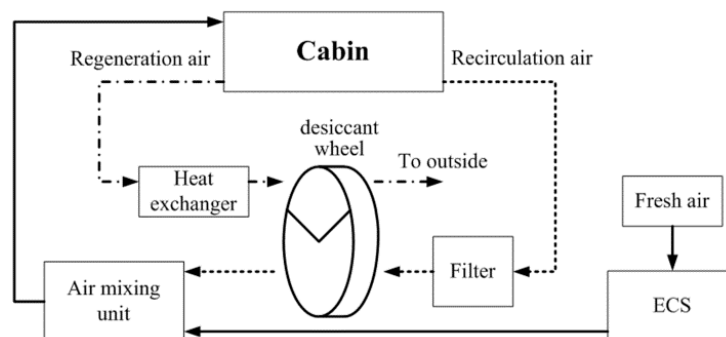


Figure 1. Desiccant wheel-based air purification system diagram.

The VOCs adsorption and desorption performances on silica gel are generally measured at equilibrium conditions, so the kinetics and the equilibrium properties are the important factors for

silica gel application. However, only a few kinetics studies on adsorption and desorption performances of silica gel have been conducted [20–22]. Most recently, the effect of silica gel microphysical properties on the moisture sorption capacity and kinetics was investigated through small-scale desiccant-coated energy exchanger experiments by Fathieh et al. [20]. Furthermore, they conducted a novel transient thermal response test on a silica gel-packed bed to release the convective heat transfer coefficient, which provided a reference for the packed bed design with porous materials [21]. The transient numerical model of both heat and moisture transfer in a thin silica gel-packed bed was developed by Kafui [22]. Their studies offered a great help for the affinity study of adsorption on silica gel. In this paper, thermogravimetric analysis (TGA) experiments were conducted to investigate the performance and kinetics of adsorption and desorption of silica gel. Three contaminants are considered in our study. They are carbon dioxide (primarily considered in a closed and crowded cabin), methane (leakage of fuel oil and slide oil could generate various alkane steams [23]), and toluene (high-toxicity gas detected in most studies [24]). Based on the measured data, the adsorption characteristics are revealed by using a Langmuir isotherm-based kinetic model. As the thermal regeneration result decides the initial concentration of adsorbate during the adsorption and desorption cycle, it is necessary to discuss the thermal regeneration process. The Van't Hoff equation, which explicates the temperature dependence of the equilibrium constant, is used to evaluate the enthalpy and entropy of thermal regeneration on silica gel. Analysis shows that the adsorption mechanism controls the silica gel adsorption processes, but both adsorption and desorption mechanisms affect the thermal regeneration process. The increase of temperature is beneficial for a desorption-terms process.

2. Materials and Methods

2.1. Adsorbent and Adsorbates

To understand the gas pollutant removal performance, a granular fine-pore silica gel (SG610-2.10, Qingdao Haiyang Chemical Co. Ltd., Qingdao, Shandong, China) was chosen as the adsorbent in this study. The physical properties of the silica gel sample were obtained through a nitrogen gas adsorption-desorption experiment at 77 K using an automatic sorption analyzer (Micromeritics ASAP2010, Micromeritics Instrument Corp., Norcross, GA, USA). Based on the Brunauer–Emmett–Teller (BET) theory, the physical properties were obtained and are listed in Table 1. Before the tests, the silica gel sample was kept in a drying vacuum oven at 393 K for at least two hours. This experimental pretreatment method can remove any impurities that might be adsorbed on the surface.

Table 1. Basic physical properties of fine-pore silica gel.

Parameters	Unit	Value
BET specific surface area	m ² /g	610
Total pore volume	cm ³ /g	0.36
Average pore size	nm	2.4
Mean particle diameter	mm	2.10

Carbon dioxide, methane, and toluene were chosen as the gas pollutants, and they were made by Beijing AP BAIF Gases Industry Co. Ltd., Beijing, China. Both carbon dioxide and methane had purities of 99.9%. Toluene was produced from a toluene/nitrogen standard gas bottle and its concentration was 609 ppm.

2.2. Experimental Apparatus and Procedure

Figure 2 shows the experiment diagram for studying the adsorption and thermal desorption kinetics for silica gel. The adsorption and desorption performances of the loaded adsorbent particle were evaluated by using a TGA analyzer (SDTA851e, Mettler Toledo GmbH., Schwerzenbach,

Switzerland) at flow rate of 100 sccm. The TGA analyzer can accurately measure the mass change of the adsorbent in these experiments. A low-temperature thermostat bath (DC-85MC, Ningbo Tianheng Instrument Factory Co. Ltd., Ningbo, China) maintained an isothermal environment. Flow rates were controlled using mass flow controllers (MC-200SCCM-D/5M-5IN, MC-50SCCM-D/5M-5IN, Alicat Scientific, Inc., Tucson, AZ, USA). The inlet concentrations of carbon dioxide and methane were monitored by using an infrared gas analyzer (GXH-3011H, Institute of Beijing HUAYUN Analytical Instrument Co. Ltd., Beijing, China). Toluene gas was supplied from a gas bottle with 609 ppm toluene/nitrogen standard gas. Prior to an adsorption run, the silica gel was heated to a temperature of 393 K for at least two hours under a stream of carrier gas. This experimental pretreatment method can remove the impurities that might be adsorbed on the surface.

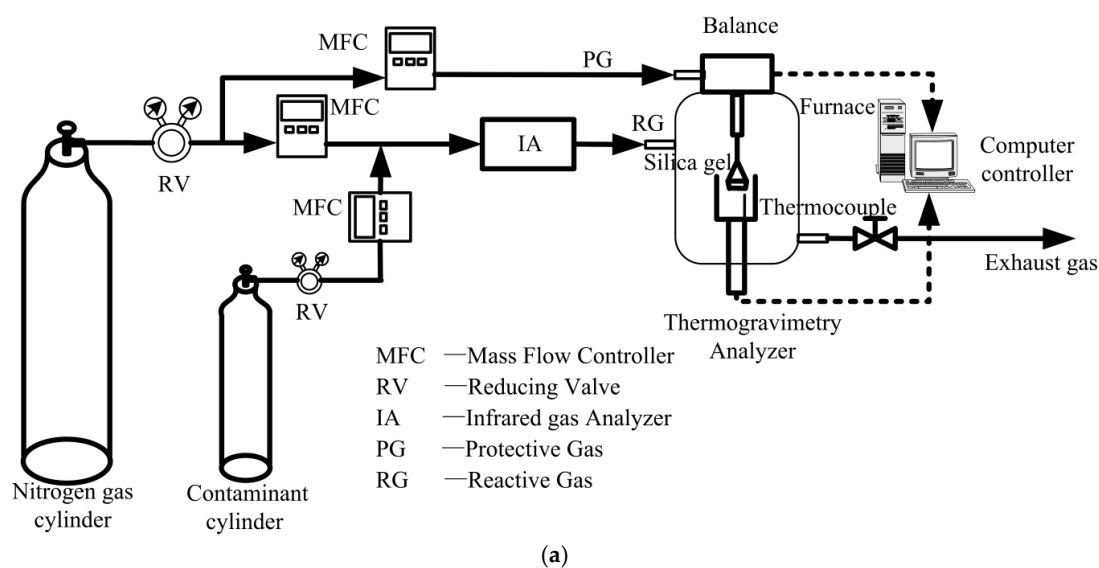


Figure 2. Experimental diagram and experimental apparatus; (a) schematic diagram of silica gel thermogravimetric analysis (TGA) experiments; (b) experimental apparatus.

Nitrogen was the carrier gas in the following adsorption experiments of silica gel. The adsorption temperature was controlled at 298 K. Three adsorption experiments were separately carried out using carbon dioxide, methane, and toluene. The concentrations of the three gas pollutants were 1000 ppm, 1000 ppm, and 609 ppm, respectively.

The thermal desorption experiments of toluene on the silica gel were conducted at three different temperatures of 313 K, 323 K, and 333 K, once the toluene adsorption reached saturation. In the thermal desorption experiments, the concentration of toluene was 609 ppm as before. The toluene concentration in the regeneration gas was employed to evaluate the feasibility of using the exhaust air regeneration.

These temperatures were employed in order to evaluate the enthalpy of desorption, which can reveal the kinetics of thermal desorption.

3. Results and Discussion

3.1. Adsorption Kinetic Model

The equilibrium adsorption performances of silica gel for carbon dioxide, methane, and toluene were obtained from the TGA experiments. Figures 3–5 show the adsorption curves for carbon dioxide, methane, and toluene as a function of time. It takes 20–30 min to reach equilibrium for carbon dioxide and methane at a concentration of 1000 ppm. In contrast, it takes about 165 min to reach equilibrium for toluene at a concentration of 609 ppm.

Some conclusions can be observed from Figures 3 and 4. The results display that a large amount of toluene was adsorbed at any given time and, at the simulated equilibrium condition, compared with methane, which may be caused by the different surface interactions. The silica gel adsorbent-toluene interaction is dominated by the hydrogen bond between the hydrogen atom bonds to the Si-OH and the aromatic delocalized pi electrons [25], which hold a much higher adsorption force than the Van der Waals force. Although the silanol groups can also interact with methane, the silica gel adsorption-methane interaction is so weak that the bands for adsorbed methane completely disappear when the temperature is over 213 K. This phenomenon was confirmed by Chen et al. [26]. Thus, the silica gel adsorbent showed a stronger affinity for toluene than methane.

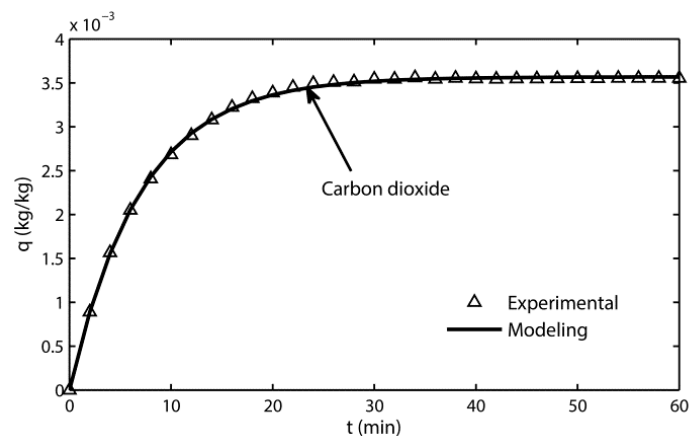


Figure 3. Experimental and modeling adsorption curves for carbon dioxide.

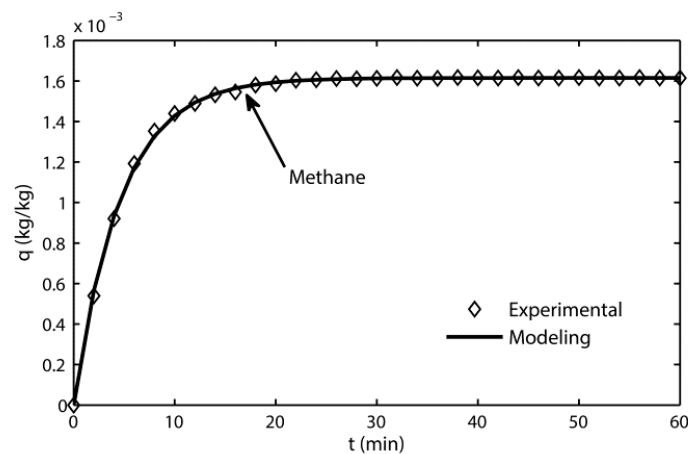


Figure 4. Experimental and modeling adsorption curves for methane.

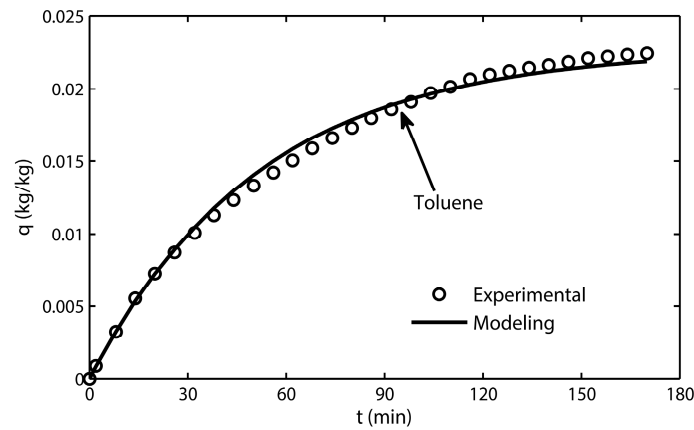


Figure 5. Experimental and modeling adsorption curves for toluene.

An appropriate kinetic model is required to understand the adsorption process and to evaluate its thermodynamics. The Langmuir isotherm is frequently assumed to comprehend the adsorptive processes [27], which considers that the adsorption and desorption of a single reaction is completely reversible. The equilibrium will be reached when the adsorption rate equals the desorption rate. The reaction is expressed as:



where P is the gas pollutant molecule in the gas phase, V is the vacant adsorption site on adsorbent solid surface, and PV implies that P is adsorbed.

The fraction of relative loading, θ , is typically calculated as:

$$\theta(t) = \frac{q(t)}{q^*} \tag{2}$$

where q is the amount of adsorbate adsorbed, kg/kg; q^* is the equilibrium amount of adsorbate adsorbed, kg/kg, and t is the time, s.

The rate of adsorption is proportional to the percentage of unoccupied active sites and the concentration of gas pollutant in the bulk flow, and the rate of desorption is proportional to the percentage of the covered surface. Thus, the rate of adsorption terms, r_a , and desorption terms, r_d , may be written as [27]:

$$r_a = k_a C(1 - \theta) \tag{3}$$

$$r_d = k_d \theta \tag{4}$$

where k_a is the reaction constant of adsorption terms, s^{-1} ; C is the concentration of gas pollutant in bulk flow and is given in molar fraction; and k_d is the reaction constant of desorption terms, s^{-1} .

Thus, the overall rate of process is:

$$r = \frac{d\theta}{dt} = k_a C(1 - \theta) - k_d \theta \tag{5}$$

For the silica gel adsorption processes described in Section 2.2, the initial condition at time t is:

$$\theta|_{t=0} = 0 \tag{6}$$

By solving Equation (5), the adsorption kinetic model can be transformed as a function of time:

$$q(t) = q^* \cdot \frac{k_a C}{k_a C + k_d} \left(1 - e^{-(k_a C + k_d)t} \right) \tag{7}$$

The fitting validity can be ensured only by ensuring adequate agreement between the kinetic model results and the experimental data. Here, the coefficient of determination, R^2 , is calculated with Equation (8):

$$R^2 = 1 - \frac{\sum_i^N (q_{exp,i} - q_{sim,i})^2}{\sum_i^N (q_{exp,i} - \bar{q}_{exp})^2} \tag{8}$$

where $q_{exp,i}$ and $q_{sim,i}$ are the amounts of adsorption under experimental and predicted conditions, respectively, \bar{q}_{exp} is the mean of experimental data, and N is the total number of fitted points.

Adsorption kinetic model errors are listed in Table 2. Every gas pollutant has unique reaction constants which can be derived from TGA experiments. These parameters are inferred and are listed in Table 2. Note that the calculated reaction constant of desorption-terms (not shown in Table 2) is less than 10^{-6} , which is low enough to ignore.

Table 2. Adsorption parameters and model errors.

Gas Pollutant	C (ppm)	k_a (s ⁻¹)	$k_a C$ (s ⁻¹)	R^2
Carbon dioxide	1000	0.240	0.0024	0.9999
Methane	1000	0.360	0.0036	0.9999
Toluene	609	0.053	0.00032	0.9903

From Table 2, we see that:

1. The adsorption-terms are the only dominant mechanism for silica gel adsorption processes at 298 K.
2. The kinetic model reflects the adsorption mechanism for silica gel because of its high fitting accuracy.

3.2. Toluene Thermal Desorption

In order to evaluate the desorption performance of silica gel, series of experiments were conducted using a concentration of 609 ppm toluene at different temperatures of 313, 323, and 333 K. Figure 6 shows curves of the fraction of relative loading with time. From Figure 6, we can observe that the thermal desorption speed was obviously affected by the operating temperature.

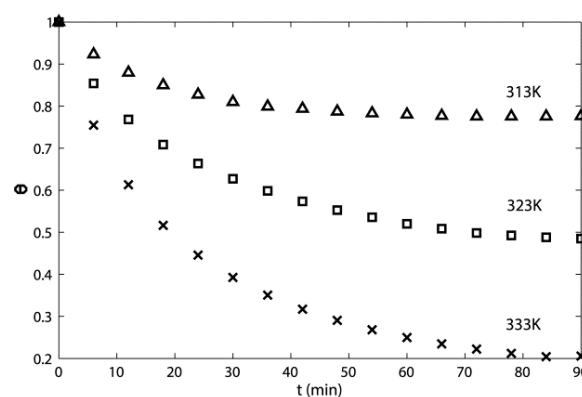


Figure 6. Toluene thermal desorption curves of silica gel.

Based on the reaction in Equation (1), the thermal desorption kinetic model can also be calculated with Equation (5). For the silica gel regeneration processes, the initial condition at time t becomes:

$$\theta|_{t=0} = 1 \tag{9}$$

By solving the difference equation of Equation (5), the thermal desorption kinetic model can be transformed into Equation (10):

$$\theta(t) = \frac{k_a C}{k_a C + k_d} + \left(1 - \frac{k_a C}{k_a C + k_d}\right) e^{-(k_a C + k_d)t} \tag{10}$$

Thus, the equilibrium relative loading, θ_e , becomes:

$$\frac{1}{\theta_e} = 1 + \frac{K}{C} \tag{11}$$

where K is the equilibrium constant, defined as $K = k_d/k_a$.

Table 3 lists the calculated reaction constants, equilibrium constant, and errors under thermal desorption conditions described in Section 2.2. The reaction constant values for the adsorption terms decrease with the increase of temperature. However, the reaction constant values for the desorption terms increase with the increase of temperature. The silica gel regeneration temperature promotes the reaction constant values to change reversely.

Table 3. Thermal desorption parameters and model errors.

Temperature (K)	$k_a C$ (s ⁻¹)	k_a (s ⁻¹)	k_d (s ⁻¹)	K	R^2
313	0.0486	7.9803	0.0141	0.00177	0.9989
323	0.0216	3.5468	0.0231	0.00651	0.9952
333	0.0108	1.7734	0.0406	0.02289	0.9955

The reaction constants are significantly influenced by temperatures, as shown in Table 3. Based on the Arrhenius equation, the reaction constant of the desorption terms reaction can be expressed in Equation (12):

$$k_d = A e^{-\frac{E_a}{RT}} \tag{12}$$

where E_a is the activation energy for the desorption-terms reaction, J/mol; A is the pre-exponential factor for the desorption-terms reaction; and R is the universal gas constant, 8.314 J/(mol·K).

The Arrhenius plot for reaction constants is shown in Figure 7, which will be used to calculate the apparent activation energy.

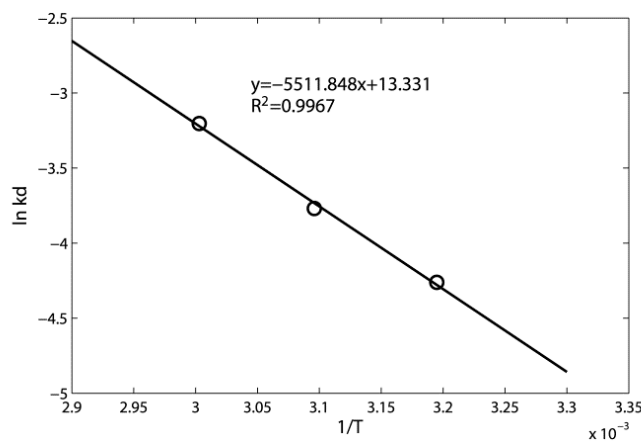


Figure 7. The Arrhenius plot for reaction constants of silica gel thermal desorption.

With Figure 7 and Equation (12), the apparent activation energy is calculated to be 45.83 kJ/mol for desorption terms. This value can reflect the difficult degree to desorb the toluene molecules from

the adsorption site of the silica gel surface. The interaction between silica gel adsorbent and toluene is very probably physical adsorption, since its apparent activation energy is lower than 83 kJ/mol, which can characterize an absorption process controlled by chemical reactions [28].

The Van't Hoff equation was used to evaluate the enthalpy of thermal desorption. Thus, the equilibrium constant is:

$$\ln K = -\frac{\Delta H}{RT} + \frac{\Delta S}{R} \quad (13)$$

where ΔH is the enthalpy of reaction, J/mol; ΔS is the entropy of reaction, J/(mol·K); and R is the universal gas constant, 8.314 J/(mol·K).

The Van't Hoff plot of equilibrium constant is shown in Figure 8, which can be used to calculate the enthalpy and entropy of the thermal desorption reaction.

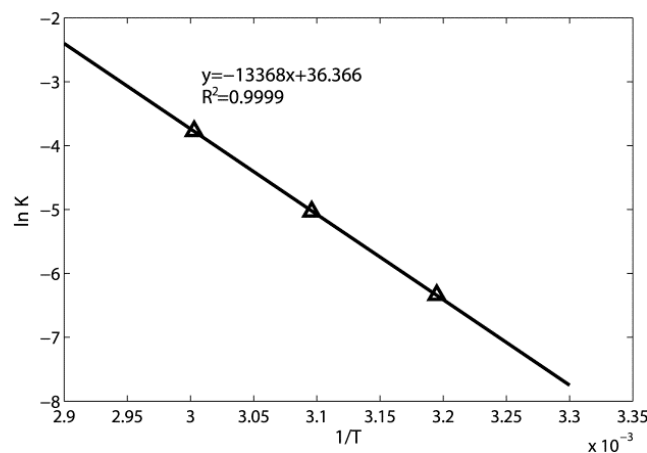


Figure 8. The Van't Hoff plot for equilibrium constant of silica gel thermal desorption.

With Figure 8 and Equation (13), the enthalpy of the reaction and the entropy of the reaction can be calculated. They are 111.14 kJ/mol and 302.35 J/(mol·K), respectively. With Equation (14), the equilibrium temperature, T_e , is 367.6 K, which indicates that the silica gel with adsorbed toluene can be entirely regenerated when it is heated to above 367.6 K:

$$\Delta H - T_e \Delta S = 0 \quad (14)$$

Therefore, the toluene regeneration process by silica gel adsorbent at equilibrium, $r = 0$, can be expressed as follows according to Equation (11):

$$\frac{1}{\theta_e} = 1 + \exp(-111.14/RT) \frac{6.22 \times 10^{15}}{C} \quad \text{for } T \in [313 \text{ K}, 333 \text{ K}] \quad (15)$$

where θ_e is the fraction of relative loading at equilibrium, C is given in molar fraction, T is given in Kelvin, and $R = 8.314 \times 10^{-3}$ kJ/(mol·K).

4. Conclusions

The potential adsorption performance and dirty purge gas desorption phenomena of granular silica gel material was investigated by TGA experiments. The kinetic model can describe the adsorption process very well for toluene, carbon dioxide, and methane at 298 K, with tiny absolute percentage deviations. The adsorption terms are certified as the only dominant mechanism for silica gel adsorption processes.

The toluene contaminant was used as the purge gas in further thermal desorption experiments. Under mixed purge gas conditions, the residual adsorbate decreased nearly linearly from 77.6% to 20.4%,

with an increase in the desorption temperature from 313 K to 333 K. The apparent activation energy for desorption-terms was 45.83 kJ/mol, obtained based on the Arrhenius equation. According to the Van't Hoff equation, the enthalpy of thermal desorption was 111.14 kJ/mol in an exothermic physical adsorption process when toluene was adsorbed on silica gel.

Acknowledgments: The authors are grateful to the anonymous reviewers for their critical and constructive review of the manuscript. Their comments helped to increase quality and readability of the manuscript. This work was supported by the Aviation Science Foundation of China (grant number 2014ZC09002).

Author Contributions: Liping Pang made substantial contributions to the conception and design; Rong A, Meng Liu and Dongsheng Yang performed the experiments and analyzed the data; Yue Zhou contributed materials analysis tools; Rong A and Liping Pang wrote the paper; Rong A, Liping Pang and Jun Wang discussed the results and implications and commented on the manuscript at all stages. The theoretical aspect of this work does not allow to point to any substantial authorship. All authors have read and approved the final manuscript.

Conflicts of Interest: The authors declare no conflict of interest.

References

1. National Research Council (U.S.). Health Surveillance. In *The Airliner Cabin Environment and the Health of Passengers and Crew*; National Academies Press: Washington, DC, USA, 2002; pp. 223–236, ISBN 0-309-56770-X.
2. Tao, H.; Meng, L.; Liping, P.; Jun, W. Studies on new air purification and air quality control system of airliner cabin. *Procedia Eng.* **2011**, *17*, 343–353. [[CrossRef](#)]
3. Bull, K. Cabin air filtration: Helping to protect occupants from infectious diseases. *Travel Med. Infect. Dis.* **2008**, *6*, 142–144. [[CrossRef](#)] [[PubMed](#)]
4. Boggia, S.; Rüd, K. Intercooled recuperated gas turbine engine concept. In Proceedings of the 41st Aiaa/Asme/Sae/Asee Joint Propulsion Conference & Exhibit, Tucson, AZ, USA, 10–13 July 2005; American Institute of Aeronautics and Astronautics: Reston, VA, USA, 2005.
5. Shim, W.G.; Kim, S.C. Heterogeneous adsorption and catalytic oxidation of benzene, toluene and xylene over spent and chemically regenerated platinum catalyst supported on activated carbon. *Appl. Surf. Sci.* **2010**, *256*, 5566–5571. [[CrossRef](#)]
6. Lillo-Ródenas, M.A.; Cazorla-Amorós, D.; Linares-Solano, A. Behaviour of activated carbons with different pore size distributions and surface oxygen groups for benzene and toluene adsorption at low concentrations. *Carbon* **2005**, *43*, 1758–1767. [[CrossRef](#)]
7. Sidheswaran, M.A.; Destailats, H.; Sullivan, D.P.; Cohn, S.; Fisk, W.J. Energy efficient indoor voc air cleaning with activated carbon fiber (acf) filters. *Build. Environ.* **2012**, *47*, 357–367. [[CrossRef](#)]
8. Liu, M.; Yang, D.S.; Pang, L.P.; Yu, Q.N.; Huang, Y. Experimental and computational investigation of adsorption performance of TC-5A and PSA-5A for manned spacecraft. *Chin. J. Aeronaut.* **2015**, *28*, 1583–1592. [[CrossRef](#)]
9. Li, G.; Pang, L.; Liu, M.; Yang, D.; Yu, Q.; Rong, A. Multiobjective optimal method for carbon dioxide removal assembly in manned spacecraft. *J. Aerosp. Eng.* **2016**, *29*, 04016052.
10. Ginestet, A.; Pugnet, D.; Rowley, J.; Bull, K.; Yeomans, H. Development of a new photocatalytic oxidation air filter for aircraft cabin. *Indoor Air* **2005**, *15*, 326–334. [[CrossRef](#)] [[PubMed](#)]
11. Sun, Y.; Fang, L.; Wyon, D.P.; Wisthaler, A.; Lagercrantz, L.; Strøm-Tejsen, P. Experimental research on photocatalytic oxidation air purification technology applied to aircraft cabins. *Build. Environ.* **2008**, *43*, 258–268. [[CrossRef](#)]
12. Wisthaler, A.; Strøm-Tejsen, P.; Fang, L.; Arnaud, T.J.; Hansel, A.; Märk, T.D.; Wyon, D.P. PTR-MS assessment of photocatalytic and sorption-based purification of recirculated cabin air during simulated 7-h flights with high passenger density. *Environ. Sci. Technol.* **2007**, *41*, 229–234. [[CrossRef](#)] [[PubMed](#)]
13. Bull, K.; Roux, P. Cabin air filtration systems—Novel technological solutions for commercial aircraft. In Proceedings of the 40th International Conference on Environmental Systems, Barcelona, Spain, 11–15 July 2010; American Institute of Aeronautics and Astronautics: Reston, VA, USA, 2010.
14. Metts, T.A. Heterogeneous reactions of ozone and d-limonene on activated carbon. *Indoor Air* **2007**, *17*, 362–371. [[CrossRef](#)] [[PubMed](#)]
15. Fang, L.; Zhang, G.; Wisthaler, A. Desiccant wheels as gas-phase absorption (gpa) air cleaners: Evaluation by ptr-ms and sensory assessment. *Indoor Air* **2008**, *18*, 375–385. [[CrossRef](#)] [[PubMed](#)]

16. Nie, J.; Fang, L.; Zhang, G.; Sheng, Y.; Kong, X.; Zhang, Y.; Olesen, B.W. Theoretical study on volatile organic compound removal and energy performance of a novel heat pump assisted solid desiccant cooling system. *Build. Environ.* **2015**, *85*, 233–242. [[CrossRef](#)]
17. Zhang, G.; He, W.; Fang, L.; Ma, F. Numerical study on the contribution of convective mass transfer inside high-porosity adsorbents in the voc adsorption process. *Indoor Built. Environ.* **2013**, *22*, 551–558. [[CrossRef](#)]
18. Zhang, G.; Zhang, Y.F.; Fang, L. Theoretical study of simultaneous water and vocs adsorption and desorption in a silica gel rotor. *Indoor Air* **2008**, *18*, 37–43. [[CrossRef](#)] [[PubMed](#)]
19. Strom-Tejsen, P.; Zukowska, D.; Fang, L.; Space, D.R.; Wyon, D.P. Advantages for passengers and cabin crew of operating a gas-phase adsorption air purifier in 11-h simulated flights. *Indoor Air* **2008**, *18*, 172–181. [[CrossRef](#)] [[PubMed](#)]
20. Fathieh, F.; Nezakat, M.; Evitts, R.W.; Simonson, C.J. Effects of physical and sorption properties of desiccant coating on performance of energy wheels. *J. Heat Transf.* **2017**, *139*, 062601. [[CrossRef](#)]
21. Naghash, M.; Fathieh, F.; Besant, R.W.; Evitts, R.W.; Simonson, C.J. Measurement of convective heat transfer coefficients in a randomly packed bed of silica gel particles using ihtp analysis. *Appl. Therm. Eng.* **2016**, *106*, 361–370. [[CrossRef](#)]
22. Kafui, K.D. Transient heat and moisture transfer in thin silica gel beds. *J. Heat Transf.* **1994**, *116*, 946–953. [[CrossRef](#)]
23. Michaelis, S. *Aviation Contaminated Air Reference Manual*; Susan Michaelis: Horsham, UK, 2007, ISBN 9780955567209.
24. Nagda, N.L.; Rector, H.E. A critical review of reported air concentrations of organic compounds in aircraft cabins. *Indoor Air* **2003**, *13*, 292–301. [[CrossRef](#)] [[PubMed](#)]
25. Ncube, T.; Kumar Reddy, K.S.; Al Shoaibi, A.; Srinivasakannan, C. Benzene, toluene, m-xylene adsorption on silica-based adsorbents. *Energy Fuels* **2017**, *31*, 1882–1888. [[CrossRef](#)]
26. Chen, L.; Lin, L.; Xu, Z.; Zhang, T.; Liang, D.; Xin, Q.; Ying, P. Interaction of methane with surfaces of silica, aluminas and HZSM-5 zeolite. A comparative FT-IR study. *Catal. Lett.* **1995**, *35*, 245–258. [[CrossRef](#)]
27. Monazam, E.R.; Spenik, J.; Shadle, L.J. CO₂ desorption kinetics for immobilized polyethylenimine (pei). *Energy Fuels* **2014**, *28*, 650–656. [[CrossRef](#)]
28. Villa, A.C.; Gutierrez, J.S.; Gomez, C.J.N.; De los Rios, G.S.A.; Villalobos, M.R.; Palacios, L.C.; Ortiz, A.L.; Collins-Martinez, V. Kinetic study of the CO₂ desorption process by carbonated Na₂ZrO₃ solid absorbent. *Int. J. Hydrog. Energy* **2015**, *40*, 17338–17343. [[CrossRef](#)]



© 2017 by the authors. Licensee MDPI, Basel, Switzerland. This article is an open access article distributed under the terms and conditions of the Creative Commons Attribution (CC BY) license (<http://creativecommons.org/licenses/by/4.0/>).